A NUMERICAL INVESTIGATION OF AN ADAPTIVE POWER SERIES APPROXIMATION TO COMPARTMENTAL MODELS*

BROOKE TORTORELLI, † AND ELLA GIGANTE ‡
PROJECT ADVISOR: DR. JOSEPH COYLE[1]

Abstract. Compartmental modeling is frequently used as a model technique when the variables of interest can be grouped into distinct categories or compartments. This is typically the case when simulating the spread and behavior of infectious diseases. When the resulting differential system is coupled in a nonlinear way, numerical techniques are often the only way to approximate the true solutions. Here, we employ a power series approximation demonstrating a way to estimate the radius of convergence as part of an adaptive technique for long term approximations.

Key words. Compartmental models, Dynamical systems, Numerical approximation, Recurrence relations, Series solutions

AMS subject classifications. 37N25, 92-08, 90C39

1. Introduction. Compartmental models are often used in simulating a phenomenon where a total population can be associated with different or mutually exclusive states at a given time. There is a long history in the development of these models related to infectious diseases. Brauer, Castillo-Chavez, and Feng [1] provide a summary of this history beginning in the seventeenth century with John Graunt's work on the study of infectious disease data. They also highlight Sir Ronald Ross' 1902 Nobel Prize (in Medicine) winning compartmental model relating mosquitoes and humans to the spread of malaria, as well as the extensive work of Kermack and McKendrick related to epidemic modelling. More recently, the interest in developing compartmental models for the study of the behavior of infectious diseases has increased, resulting in more comprehensive models.

Accompanying the model development is the need for numerical methods to approximate solutions. This paper is a study in the series solution approach and is, in some sense, an extension of [14]. Heng and Althaus [6] seek solutions in the form of what they call semi-analytic solutions. Harko, Lobo, and Mak [4] also develop semi-analytic solutions, and provide a thorough summary of other numerical approaches including variation iterative methods [5, 12] and differential transformation techniques such as in [3, 8]. Of course, techniques such as Euler's method and other more sophisticated iterative solvers associated with systems of differential equations [11] remain viable in many cases.

In Section 2, we provide a basic overview of the classical SIR model, including the development of the model and brief remarks about the equilibrium solutions. In Section 3, we develop the recurrence relations associated with the series solutions for the basic model and provide a detailed algorithm for implementation. Then, in Section 4, we provide several numerical results culminating in a demonstration of the effectiveness of the algorithm.

*Submitted to the editors February 10, 2026.
Funding: This work was funded by the Monmouth University School of Science Summer Research Program.
†Monmouth University, West Long Branch, NJ (s1305131@monmouth.edu).
‡Middletown North High School, Middletown, NJ (egigante16@gmail.com).
[0]Monmouth University, West Long Branch, NJ (jcoyle@monmouth.edu)

2. The SIR Model. In this section, we consider a basic model for the development of the series solutions. A more sophisticated model will be employed in the numerical investigation that follows. Construction of the model begins by partitioning a population of size N into three categories [13] for a time, t :

S(t) = number of susceptible individuals,
I(t) = number of infectious individuals, and
R(t) = number of recovered individuals.

Typically, these quantities are normalized by setting

$$s(t) = \frac{S(t)}{N},\ i(t) = \frac{I(t)}{N},\ \text{and}\ r(t) = \frac{R(t)}{N} \tag{2.1}$$

to represent the fraction of the total population in each group. Note that since our population is fixed, we have

$$s(t) + i(t) + r(t) = 1. \tag{2.2}$$

The relationship between the groups is better defined by the relationship between populations and their rates of change. Following [9], we first introduce a few constants:

β = fixed number of contacts per infected individuals per day,
γ = fixed number of the infected group recovering from the disease, and
μ = fixed number of the infected group recovering from the disease.

This leads to the following SIR model:

$$\frac{ds}{dt} = -\beta s(t)i(t) + \eta r(t), \tag{2.3}$$

$$\frac{di}{dt} = \beta s(t)i(t) - \gamma i(t), \tag{2.4}$$

$$\frac{dr}{dt} = \gamma i(t) - \eta r(t) \tag{2.5}$$

with appropriate initial conditions at some initial time, t_0: $s(t_0)$, $i(t_0)$, and $r(t_0)$.

3. Series Solutions. In this section we provide, for completeness, the development of the series solution and associated recurrence relations for the coefficients. In addition, an adaptive algorithm for the implementation is presented.

3.1. Recurrence Relations. As in [14], we seek a series solution. Let $\{s_n\}_{n=0}^{\infty}$, $\{i_n\}_{n=0}^{\infty}$, and $\{r_n\}_{n=0}^{\infty}$ be power series coefficients such that

$$s(t) = \sum_{n=0}^{\infty} s_n(t-t_0)^n,\quad i(t) = \sum_{n=0}^{\infty} i_n(t-t_0)^n,\ \text{and}\ r(t) = \sum_{n=0}^{\infty} r_n(t-t_0)^n \tag{3.1}$$

where $s(0) = s_0, e(0) = e_0, i(0) = i_0,$ and $r(0) = r_0$. We assume $t_0 = 0$ and substitute these forms into the system (2.3) - (2.5) to get

$$\begin{aligned}\frac{ds}{dt} = \sum_{n=0}^{\infty} s_n n t^{n-1} &= -\beta \left(\sum_{n=0}^{\infty} s_n t^n\right)\left(\sum_{n=0}^{\infty} i_n t^n\right) + \eta \sum_{n=0}^{\infty} r_n t^n \\ &= -\beta \sum_{n=0}^{\infty}\left(\sum_{k=0}^{n} s_k i_{n-k} t^n\right) + \eta \sum_{n=0}^{\infty} r_n t^n,\end{aligned}$$

or,

$$\sum_{n=0}^{\infty} s_{n+1}(n+1)t^n = -\beta \sum_{n=0}^{\infty}\left(\sum_{k=0}^{n} s_k i_{n-k} t^n\right) + \eta \sum_{n=0}^{\infty} r_n t^n.$$

Similarly,

$$\sum_{n=0}^{\infty} i_{n+1}(n+1)t^n = \beta \sum_{n=0}^{\infty}\left(\sum_{k=0}^{n} s_k i_{n-\eta} t^n\right) - \gamma \sum_{n=0}^{\infty} i_n t^n$$

and

$$\sum_{n=0}^{\infty} r_{n+1}(n+1)t^n = \gamma \sum_{n=0}^{\infty} i_n t^n - \eta \sum_{n=0}^{\infty} r_n t^n.$$

This leads to the following recursive definition of the coefficients for $n \geq 0$:

$$s_{n+1} = \frac{1}{n+1}\left(-\beta \sum_{k=0}^{n} s_k i_{n-k} + \eta r_n\right), \tag{3.2}$$

$$i_{n+1} = \frac{1}{n+1}\left(\beta \sum_{k=0}^{n} s_k i_{n-k} - \gamma i_n\right), \tag{3.3}$$

and

$$r_{n+1} = \frac{1}{n+1}\left(\gamma i_n - \eta r_n\right). \tag{3.4}$$

3.2. Implementation. As is suggested in [14], implementation requires a restart (or re-centering) of the series and and thoughtful, yet practical, choice of N. Consequently, we set

$$s(t, t', N) = \sum_{n=0}^{N} s_{t',n}(t - t')^n, \tag{3.5}$$

and similarly define $i(t, t', N)$ and $r(t, t', N)$. The choice of distance between consecutive t'-values is central to the success of the implementation. It is essential to determine a radius of convergence for each of the series representations on intervals whose minimum value is t'. We denote this interval by

$$\mathcal{I}_{t',\varepsilon} = [t', t' + \varepsilon]. \tag{3.6}$$

Given the lack of explicit formulae for the coefficients and noting that typically not all terms are positive, we consider the series of positive terms,

$$\sum_{n=0}^{N} |s_{t',n}|(t-t')^n, \tag{3.7}$$

and seek values of c and b for which

$$|s_{t',n}| \sim c\mathrm{e}^{bn}. \tag{3.8}$$

The quality of this relationship will be illustrated in the next section. Given suitable values for c and b, and for t satisfying $|t-t'| < \epsilon e^{-b}$, we note the ratio

$$\left|\frac{s_{t',n+1}}{s_{t',n}}\right| \approx \left|\frac{ce^{b(n+1)}(t-t')^{n+1}}{ce^{bn}(t-t')^n}\right| = \mathrm{e}^b|t-t'| < \epsilon \tag{3.9}$$

indicates the series will converge for an ε value generally less than e^{-b}. This is based on the assumption that the approximation in (3.8) is reasonable. We should be cautious in terms of what is used in practice based on the fact that the series will be truncated.

Consider, for example, the classic power series representation centered at $x_0 = 0$

$$\frac{1}{1-x} = \sum_{n=0}^{\infty} x^n, \tag{3.10}$$

which is valid for $x \in (-1, 1)$. That is to say, the radius of convergence is 1. However, employing (3.10) requires a truncation of the series which significantly impacts the useful radius of convergence. This is illustrated in Figure 1 where we see the series in (3.10) truncated using $N = 15, 30$, and 45 compared to the true solution in an interval of the form $(-1, -1+\delta)$ for some $\delta > 0$. It should be noted that even with $N = 45$, there is a significant lack of approximation near the end of the interval of convergence. In light of this observation, we consider ε to be an upper bound with the understanding that quality approximations will likely require a smaller interval length.

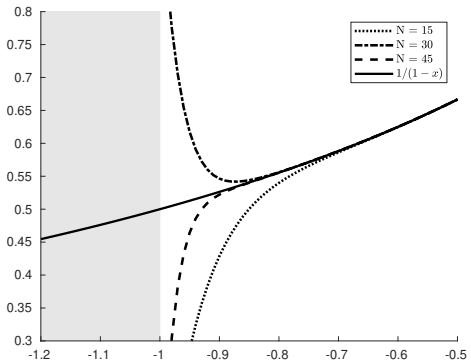

FIG. 1. *The series in (3.10) truncated using* $N = 15, 30,$ *and* 45 *compared to the true solution in an interval around* $x = -1$. *The grey area represents the limit beyond the theoretical interval of convergence which is* $(-1, 1)$.

In order to approximate values of s, i, and r on a global or total interval,

$$\mathcal{T} = [t_0, t_{end}], \tag{3.11}$$

we propose the following adaptive procedure given in Algorithm 3.1.

Algorithm 3.1 Adaptive Algorithm - fixed N-value:

(0) Choose a truncation value, N, for the series in (3.1), determine a method for choosing the length of each subinterval, ε in $\mathcal{I}_{t',\varepsilon}$, and initialize $t' = t_0$.

Then, until $t' \geq t_{end}$, repeat steps $(1) - (4)$:

(1) Compute coefficients in the recurrence relations (3.2) - (3.4) with initial conditions $s(t'), i(t')$, and $r(t')$.

(2) Compute ε for $\mathcal{I}_{t',\varepsilon}$.

(3) Compute the values of $s(t, t', N), i(t, t', N)$, and $r(t, t', N)$ for $t \in \mathcal{T} \cap \mathcal{I}_{t',\varepsilon}$.
(4) Set t' the right end point of $\mathcal{I}_{t',\varepsilon}$ in (3).

In light of potentially poorer approximation by the truncated series near the end of each sub-interval, in what follows we demonstrate a few particular aspects of employing a series approximation and provide a numerical example implementing this algorithm where ε is chosen based on (3.9).

4. Numerical Results. In this section, we provide a series of numerical examples beginning with a benchmark true solution followed by a few that focus on nuances of the implementation, and finally, the implementation of the adaptive algorithm.

4.1. Benchmark Solution. In order to assess the accuracy of the scheme, we set our *true* solution to be the approximation obtained by employing Euler's method. Consider the general system of M first-order differential equations and initial conditions given by

$$y_i'(y_1, ..., y_M) = f_i(t, y_1, ..., y_M), \tag{4.1}$$

with initial conditions

$$y_i(t_0) = y, \tag{4.2}$$

for $i = 1, ..., M$. In vector form, (4.1) is

$$\boldsymbol{y}' = \boldsymbol{f}(\boldsymbol{y}), \tag{4.3}$$

where

$$\boldsymbol{y} = \begin{bmatrix} y_1 \\ y_2 \\ \vdots \\ y_M \end{bmatrix} \text{ and } \boldsymbol{f}(\boldsymbol{y}) = \begin{bmatrix} f_1(y_1, ..., y_M) \\ f_2(y_1, ..., y_M) \\ \vdots \\ f_M(y_1, ..., y_M) \end{bmatrix}.$$

The initial condition in (4.2) can then take the form

$$\boldsymbol{y}(t_0) = \begin{bmatrix} y_1(t_0) \\ y_2(t_0) \\ \vdots \\ y_M(t_0) \end{bmatrix}.$$

If the model is discretized over time, where t is the number of days since t_0, then we may uniformly partition the time interval of interest, $\mathcal{T}$, by setting

$$t_i = t_0 + ih. \tag{4.4}$$

For simplicity, we consider an h-value of the form $10^{-p}, p \in \mathbb{N}$. Setting $\boldsymbol{y}_i = \boldsymbol{y}(t_i)$ and, using $\boldsymbol{Y}_i$ to denote the approximation of $\boldsymbol{y}_i$, we implement the basic Euler's method for systems of differential equations as

$$\boldsymbol{Y}_{i+1} = \boldsymbol{Y}_i + h\boldsymbol{f}(\boldsymbol{Y}_i), \tag{4.5}$$

where $\boldsymbol{Y}_0 = \boldsymbol{y}(t_0)$. In the case of (2.3) - (2.5), we have

$$\boldsymbol{y} = \begin{bmatrix} s \\ i \\ r \end{bmatrix} \text{ and } \boldsymbol{f}(\boldsymbol{y}) = \begin{bmatrix} -\beta si + \eta r \\ \beta si - \gamma i \\ \gamma i - \eta r \end{bmatrix}.$$

Specifically, to obtain a *true* solution, we implement (4.5) with a step size $h = 10^{-8}$ and retain the outputs corresponding to $t \in \mathbb{W}$ where we denote the vector of outputs $\boldsymbol{S}_T$, $\boldsymbol{I}_T$, and $\boldsymbol{R}_T$, respectively.

In order to quantify the accuracy between the true solution and the calculated series solution, we define the (relative) error to be

$$\boldsymbol{E} := \max\left\{ \frac{|\boldsymbol{S}_T - \boldsymbol{s}|}{|\boldsymbol{S}_T|}, \frac{|\boldsymbol{I}_T - \boldsymbol{i}|}{|\boldsymbol{I}_T|}, \frac{|\boldsymbol{R}_T - \boldsymbol{r}|}{|\boldsymbol{R}_T|} \right\}, \tag{4.6}$$

where we denote the calculated series solutions as $\boldsymbol{s}$, $\boldsymbol{i}$, and $\boldsymbol{r}$, respectively. Note that in this case $\boldsymbol{E}$ depends on N and ε. We hope to offer insight into this dynamic in the following examples.

4.2. Single Interval. The first example is a numerical investigation into the dynamics related to the choice of N and ε. In particular, we set $\beta = \frac{1}{4}, \gamma = \frac{1}{7}$, and $\eta = \frac{1}{90}$ and consider a single, initial, interval $[0, \varepsilon]$. Initially, using (3.2) - (3.4) to compute the first 61 ($N = 60$) coefficients, we use standard linear regression to determine c and ε in (3.8) for the three sets of coefficients associated with s, i, and r. The plots of the coefficients and the regression line of best fit are shown together in Figure 2(a). Here, we see that the values for b are $-2.7744, -2.7753$, and -2.8189, for s, i, and r, respectively. Consequently, we may expect to see quality convergence results for choices of ε as $16.0291, 16.0443$, and 16.7545, respectively. The plots of the series solutions for $N = 15, 30$, and 45 together with the associated true solutions are shown in Figure 2(b) $-$ (d) where in each case the limit for ε is indicated by the gray shading beyond. In each case, it is evident that as N increases, the better approximation improves. These examples also further support the notion that a practical choice for ε should be less than the approximation of e^{-b}.

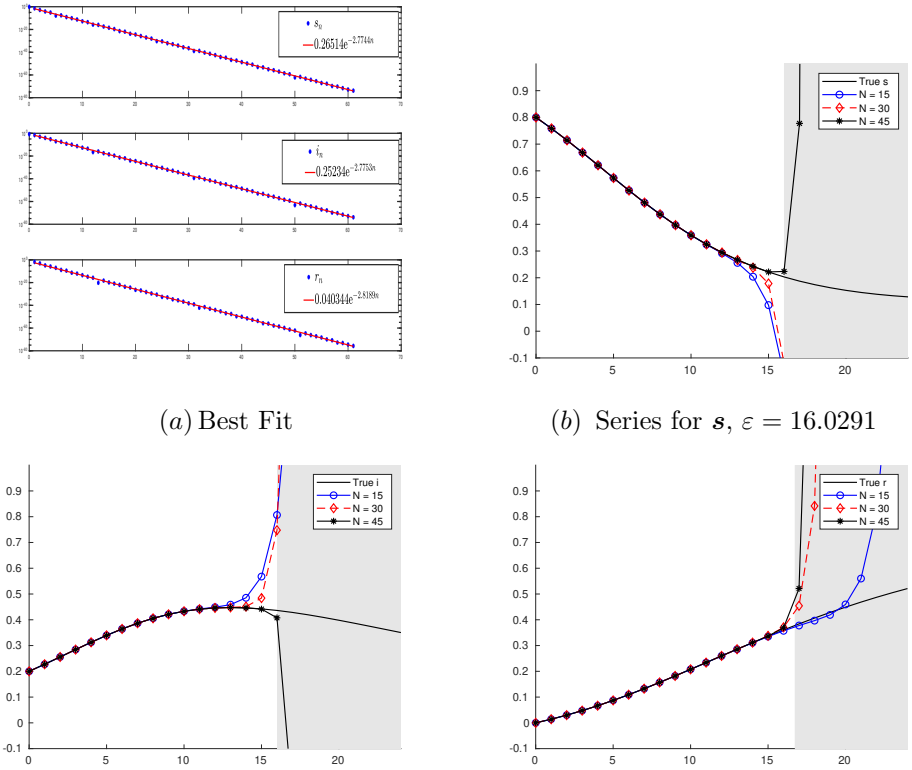

(a) Best Fit (b) Series for $\boldsymbol{s}$, $\varepsilon = 16.0291$

(c) Series for $\boldsymbol{i}$, $\varepsilon = 16.0443$ (d) Series for $\boldsymbol{r}$, $\varepsilon = 16.7545$

FIG. 2. *The coefficients and the best fit are shown for $N = 60$ for $s, i,$ and r in (a). The plots of the series solutions for $N = 15, 30,$ and 45 together with the associated true solutions are shown in $(b) - (d)$.. In each case, ε is indicated by the gray shading beyond.*

4.3. Weighted Residual Method Comparison. In this section we compare the results of the previous example with a method of weighted residuals. The connection lies in the choice of trial functions, $\{t^i\}_{i=0}^N$. To this end, we assume that $s, i,$ and r take the same form as in (3.1). Inserting into (2.3) yields

$$\begin{aligned}\sum_{p=1}^{N} p s_p t^{p-1} &= -\beta\left(s_0 i_0 + s_0 \sum_{p=1}^{N} i_p t^p + i_0 \sum_{p=1}^{N} s_p t^p\right) \\ &\quad -\beta\left(\sum_{p=1}^{N} s_p t^p\right)\left(\sum_{p=1}^{N} i_p t^p\right) + \eta\left(r_0 + \sum_{p=1}^{N} r_p t^p\right),\end{aligned}$$

which leads to

$$\begin{aligned}&\sum_{p=1}^{N} p s_p t^{p-1} + \beta s_0 \sum_{p=1}^{N} i_p t^p + \beta i_0 \sum_{p=1}^{N} s_p t^p - \eta \sum_{p=1}^{N} r_p t^p \\ &\qquad + \beta\left(\sum_{p=1}^{N} s_p t^p\right)\left(\sum_{p=1}^{N} i_p t^p\right) = -\beta s_0 i_0 + \eta r_0. \qquad (4.7)\end{aligned}$$

Similarly, inserting the forms for $s(t), i(t)$, and $r(t)$ into (2.4) and (2.5) yields

$$\begin{aligned} -\sum_{p=1}^{N} \beta i_0 s_p t^p \quad &+ \quad \sum_{p=1}^{N} i_p(-\beta s_0 t^p + p t^{p-1}) + \sum_{p=1}^{N} \gamma i_p t^p \\ &- \quad \beta \left(\sum_{p=1}^{N} s_p t^p \right) \left(\sum_{p=1}^{N} i_p t^p \right) = \beta s_0 i_0 - \gamma i_0, \end{aligned} \tag{4.8}$$

and

$$-\sum_{p=1}^{N} \gamma i_p t^p + \sum_{p=1}^{N} r_p(\eta t^p + p t^{p-1}) = \gamma i_0 - \eta r_0, \tag{4.9}$$

respectively. Defining $v_i(t) = t^{i-1}$, for $i = 1, ..., N$, multiplying (4.7) by v_i, and integrating over $[0, t']$ for some $t' > 0$ yields

$$\begin{aligned} \sum_{p=1}^{N} s_p \left(\beta i_0 \int_{t_0}^{t'} t^{p+i-1} dt + \int_{t_0}^{t'} p t^{p+i-2} dt \right) + \sum_{p=1}^{N} i_p \beta s_0 \int_{t_0}^{t'} t^{p+i-1} dt - \sum_{p=1}^{N} r_p \eta \int_{t_0}^{t'} t^{p+i-1} dt \\ + \sum_{m=1}^{N} \sum_{n=1}^{N} i_m s_n \int_{t_0}^{t'} t^{m+n+i-1} dt = (-\beta s_0 i_0 + \eta r_0) \int_{t_0}^{t'} t^{i-1} dt. \end{aligned}$$

leads to the following (nonlinear) functions for coefficients $\{s_p\}, \{i_p\}, \{r_p\}$, $p = 1, ..., N$ (denoted as vectors $\boldsymbol{s}, \boldsymbol{i}$, and $\boldsymbol{r}$, respectively)

$$\begin{aligned} f_{1,i}(\boldsymbol{s}, \boldsymbol{i}, \boldsymbol{r}) := \sum_{p=1}^{N} (\beta i_0 \boldsymbol{M}_{p,i} + \boldsymbol{D}_{p,i}) s_p \quad &+ \quad \sum_{p=1}^{N} \beta s_0 \boldsymbol{M}_{p,i} i_p - \sum_{p=1}^{N} \eta \boldsymbol{M}_{p,i} r_p + \beta \sum_{m=1}^{N} \sum_{n=1}^{N} i_m s_n \boldsymbol{G}_{m,n,i} \\ &- \quad (\gamma r_0 - \beta s_0 i_0) \boldsymbol{v}_i = 0, \end{aligned}$$

for $i = 1, .., N$ where we define the two $N \times N$ matrices

$$\boldsymbol{M}_{p,i} = \int_{t_0}^{t'} t^{p+i-1} dt, \ p, i = 1, ..., N$$

and

$$\boldsymbol{D}_{p,i} = \int_{t_0}^{t'} p t^{p+i-2} dt, \ p, i = 1, ..., N,$$

the $N \times 1$ column vector

$$\boldsymbol{v}_m = \int_{t_0}^{t'} t^{m-1}, \ m = 1, ..., N,$$

and the $N \times (2N - 1)$ matrix

$$\boldsymbol{G}_{m,n,i} = \int_{t_0}^{t'} t^{m+n+i-1} dt, \ m, n, i = 1, ..., N.$$

Similarly,

$$f_{2,i}(\boldsymbol{s},\boldsymbol{i},\boldsymbol{r}) := \sum_{p=1}^{N} -\beta i_0 \boldsymbol{D}_{p,i} s_p \quad + \quad \sum_{p=1}^{N} \left((\gamma - \beta s_0)\boldsymbol{M}_{p,i} + \boldsymbol{D}_{p,i}\right) i_p - \beta \sum_{m=1}^{N}\sum_{n=1}^{N} i_m s_n \boldsymbol{G}_{m,n,i} \\ - \quad (\beta s_0 i_0 + \gamma i_0) v_i = 0,$$

and

$$f_{3,i}(\boldsymbol{s},\boldsymbol{i},\boldsymbol{r}) := \sum_{p=1}^{N} \gamma \boldsymbol{D}_{i,p} i_p - \sum_{p=1}^{N} (\boldsymbol{D}_{i,p} - \eta \boldsymbol{M}_{i,p}) r_p - (\gamma i_0 - \eta r_0) v_i = 0,$$

for $i = 1, .., N$.

Defining $\boldsymbol{v} = [\boldsymbol{s}, \boldsymbol{i}, \boldsymbol{r}]^{\mathsf{T}}$, $\boldsymbol{F} = [f_{1,1}, ..., f_{1,N}, f_{2,1}, ..., f_{2,N}, f_{3,1}, ..., f_{3,N}]^{\mathsf{T}}$, and setting some initial approximation as $\boldsymbol{v}^{(0)}$, we employ Newton's iterative method, for example see [7], which is

$$\boldsymbol{v}^{(k)} = \boldsymbol{v}^{(k-1)} - \boldsymbol{J}^{-1}(\boldsymbol{v}^{(k-1)})\boldsymbol{F}(\boldsymbol{v}^{(k-1)})$$

for $k = 1, ..., M$ for some positive integer M where

$$\boldsymbol{J} = \begin{bmatrix} (\beta i_0 \boldsymbol{M} + \boldsymbol{D}) + \beta \boldsymbol{R_s} & \beta s_0 \boldsymbol{M} + \beta \boldsymbol{R_i} & -\eta \boldsymbol{M} \\ -\beta i_0 \boldsymbol{D} - \beta \boldsymbol{R_s} & (\gamma - \beta s_0)\boldsymbol{M} + \boldsymbol{D} - \beta \boldsymbol{R_i} & \boldsymbol{0} \\ \boldsymbol{0} & \gamma \boldsymbol{D} & -(\boldsymbol{D} - \eta \boldsymbol{M}) \end{bmatrix},$$

where

$$[\boldsymbol{R_s}]_{ij} = \frac{\partial}{\partial s_k}\left(\sum_{m=1}^{N}\sum_{n=1}^{N} i_m s_n \boldsymbol{G}_{m,n,i}\right) = s_k \sum_{m=1}^{N} i_m \boldsymbol{G}_{m,k,i},$$

and

$$[\boldsymbol{R_i}]_{ij} = \frac{\partial}{\partial i_k}\left(\sum_{m=1}^{N}\sum_{n=1}^{N} i_m s_n \boldsymbol{G}_{m,n,i}\right) = i_k \sum_{n=1}^{N} s_n \boldsymbol{G}_{k,n,i}.$$

Here, we employ the same parameters as in the previous example: $\beta = \frac{1}{4}, \gamma = \frac{1}{7}$, and $\eta = \frac{1}{90}$. In Figure 5(a) we plot the relative error of the first N coefficients calculated with the recursion formulas in (3.2)-(3.4) as the true solution and those values computed by the weighted residual method using the interval $[0, t' = 8]$ and $M = 20$. We denote the error in each case as the coefficients computed by the weighted residual method appear to degrade as the order increases. In Figure 5(b), we again calculate the coefficients for s, i and r using (3.2) - (3.4) and compute $\|\boldsymbol{F}\|/\|\boldsymbol{v}\|$. Here we show the results for $N = 1, ..., 10$ and three different intervals with $t_0 = 0$ and $t' = 4, 8, 12$..

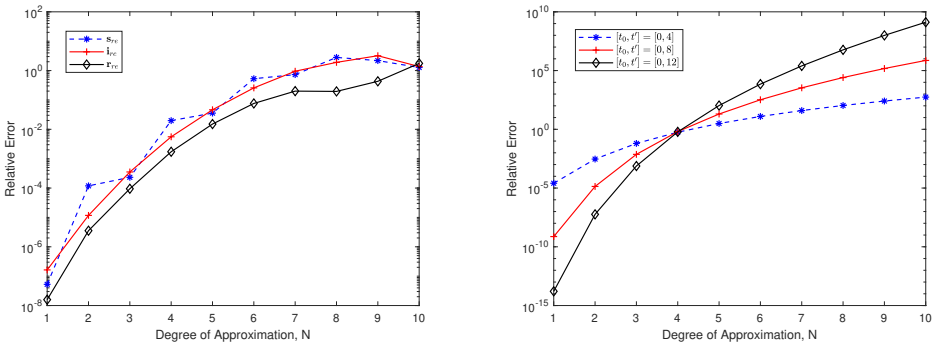

(a) (b)

FIG. 3. *In (a) we see the relative error of the first N coefficients using the interval $[0, t' = 8]$ and $M = 20$. The coefficients computed by the weighted residual method appear to degrade as the order increases. In Figure 5(b), we computed the coefficients for s, i and r again using (3.2) - (3.4) and compute $\|\boldsymbol{F}\|/\|\boldsymbol{v}\|$. Here we show the results for $N = 1, ..., 10$ and three different intervals with $t_0 = 0$ and $t' = 4, 8, 12$.*

4.4. Multiple Intervals Over Extended Time Frame. In this example, we demonstrate the implementation of the algorithm without the adaptive choice of ϵ in step (3) using fixed values of N and ε. We continue with the parameters set in the previous example and consider a time frame from $t = 0$ to $t = 1000$. The algorithm is run for ε-values of $11, 10, 9$, and 8, each for N-values beginning with $2, 5$ and then in increments of 5 to 60. The results for $\varepsilon = 8$ and $N = 45$ are shown in Figure 4(a). The convergence of the error $\mathbf{E}$ in (4.6) is shown in Figure 4(b) where the results are intuitive in the sense that the error decreases as both ε decreases and N increases.

The equilibrium values [11] of the systems are the values for which $\boldsymbol{f}(\boldsymbol{v}) = \mathbf{0}$. For our SIR system, (2.3) - (2.5), we obtain, aside from the origin $(0, 0, 0)$, and the disease free equilibrium solution, $\boldsymbol{e}_{df} = (1, 0, 0)$,

$$\boldsymbol{e}_{eq} = (e_s, e_i, e_r) = \left(\frac{\gamma}{\beta}, \frac{\gamma(\beta - \gamma)}{\beta(\eta + \gamma)}, \frac{\eta(\beta - \gamma)}{\beta(\eta + \gamma)}\right). \tag{4.10}$$

In this example, $e_s = 0.6, e_i = 0.386$, and $e_r = 0.016$. The stability of the equilibrium solution is similar to the analysis of the more sophisticated model found in [2]. We assess the quality of reaching the equilibrium solutions using the series approximation by considering large values of t_{end}. The relative error between the computed and true equilibrium values are shown in Tables 1 and 2 ($t_{end} = 1,000$ and $2,000$, respectively) for fixed ε values of $13, 12$, and 6, where in each case we compare the errors for $N = 5$ and 40. In general the results appear to show that, for larger t, there is little difference between the two choices of N.

4.5. SEIR Model and Adaptive Algorithm. In this example, we employ a more complex model by adding a group that represents those that have been exposed, but are not yet infectious. Consequently, as in [10], we introduce the constant, μ, to

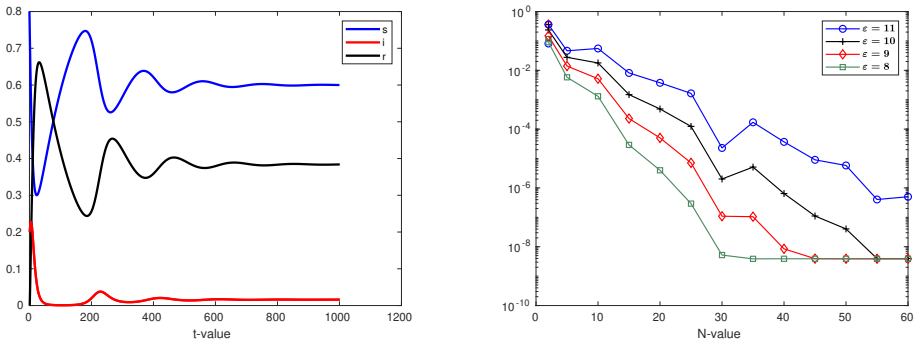

(a) $\varepsilon = 8$ and $N = 45$ (b) N vs $\mathbf{E}$

FIG. 4. *The computed series results for $\varepsilon = 8$ and $N = 45$ are shown in (a). The convergence of the error $\mathbf{E}$ in (4.6) is shown in (b) where the results are intuitive in the sense that the error decreases as both ε decreases and N increases.*

TABLE 1

The relative error between the computed and true equilibrium values for fixed ϵ and N-values . The results are shown for $t_{end} = 1000$.

ε	N	Rel. Error s	Rel. Error i	Rel. Error r
13	5	3.675 e−4	5.597 e−3	8.074 e−4
	40	1.443 e−4	4.769 e−3	2.681 e−5
12	5	2.608 e−5	5.473 e−3	6.356 e−4
	40	3.611 e−6	5.102 e−3	1.562 e−4
6	5	3.137 e−5	5.115 e−3	1.641 e−4
	40	3.224 e−5	5.112 e−3	1.626 e−4

represent the loss of latency. The new system is then written as

$$\frac{ds}{dt} = -\beta si + \eta r, \tag{4.11}$$

$$\frac{de}{dt} = \beta si - \mu e, \tag{4.12}$$

$$\frac{di}{dt} = \mu e - \gamma i, \tag{4.13}$$

$$\frac{dr}{dt} = \gamma i - \eta r. \tag{4.14}$$

Similarly to the SIR model, a recursive definition of the coefficients for $n \geq 0$ is easily constructed where we find

$$\begin{aligned} s_{n+1} &= \frac{1}{n+1}\left(-\beta \sum_{k=0}^{n} s_k i_{n-k} + \eta r_n\right), \\ e_{n+1} &= \frac{1}{n+1}\left(\beta \sum_{k=0}^{n} s_k i_{n-k} - \mu e_n\right), \\ i_{n+1} &= \frac{1}{n+1}\left(\mu e_n - \gamma i_n\right), \end{aligned}$$

TABLE 2
The relative error between the computed and true equilibrium values for fixed ϵ and N-values. The results are shown for $t_{end} = 2000$.

ε	N	Rel. Error s	Rel. Error i	Rel. Error r
13	5	8.970 e−8	5.568 e−6	1.170 e−6
	40	8.416 e−7	1.925 e−6	1.235 e−6
12	5	8.937 e−5	4.838 e−6	1.195 e−6
	40	8.802 e−6	2.789 e−6	1.259 e−6
6	5	8.815 e−7	2.825 e−6	1.260 e−6
	40	8.818 e−7	2.818 e−6	1.259 e−6

and

$$r_{n+1} = \frac{1}{n+1}\Big(\gamma i_n - \eta r_n\Big).$$

In this example, we set $\beta = \frac{1}{3}, \eta = \frac{1}{60}, \gamma = \frac{1}{8}$ and $\mu = \frac{1}{12}$ and, initially, provide results

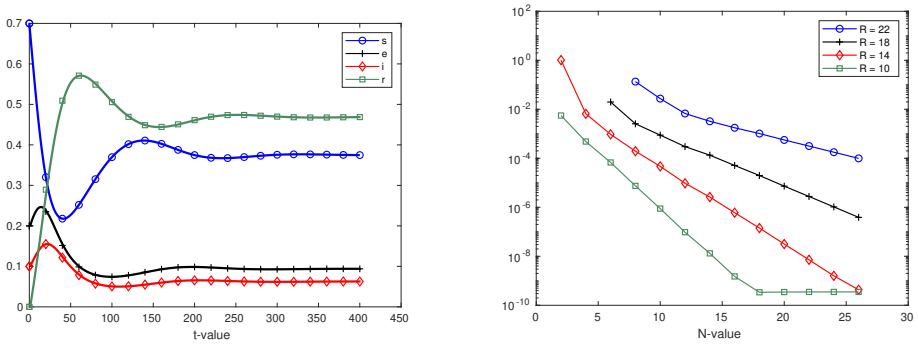

(a) (b)

FIG. 5. *Computational results for the SEIR example for $t = 0$ to $t = 400$ are shown in (a).*

similar to the previous example and Figure 4. The results, shown in Figure 6, are similar and consistent in that we see a better, or more accurate, result with increased N and decreased ε. Note here that the error (4.6) is now the maximum that includes $\boldsymbol{e}$.

The algorithm is performed for three fixed values of $N = 25, 35$, and 45 where, for each N, the algorithm is run for $p = 1, 0.9, 0.8, 0.7$, and 0.6. The results are shown in Figure 6 where we illustrate the length of each consecutive interval and relative error of the computation for $t \in [0, 400]$. The results are consistent with expectations in that we see smaller (and more) sub-intervals for smaller p-values with more accuracy.

Next, we employ the adaptive algorithm from Section 3.2. For each t', we determine $\mathrm{e}^{-b_s}, \mathrm{e}^{-b_e}, \mathrm{e}^{-b_i}$, and e^{-b_r}, for the four series and then set

$$\varepsilon = p \min\left\{\mathrm{e}^{-b_s}, \mathrm{e}^{-b_e}, \mathrm{e}^{-b_i}, \mathrm{e}^{-b_r}\right\} \tag{4.15}$$

where $p \in (0, 1]$. The inclusion of p is based on the knowledge that (3.8) is an approximation and that the series will be truncated.

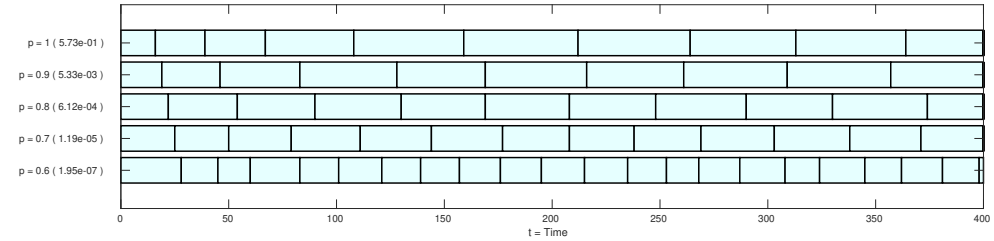

$(a)\ N = 25$

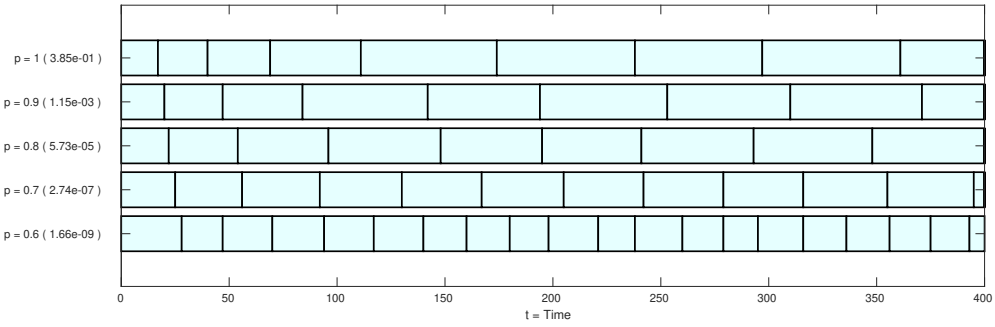

$(b)\ N = 35$

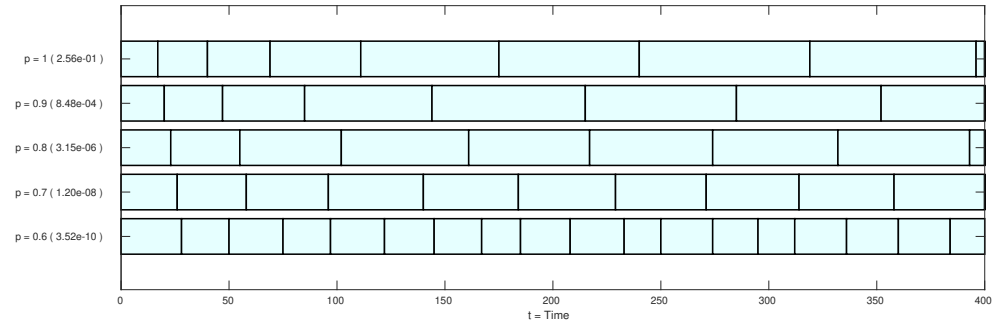

$(c)\ N = 45$

FIG. 6. *Each of the three figures above displays the length of ε for each subinterval found at each step of the algorithm for values of $p = 1, 0.9, 0.8, 0.7,$ and 0.6. Specifically, $N = 25, 35,$ and 45, in $(a), (b),$ and (c), respectively. We observe smaller (and more) subintervals for smaller p-values with more accuracy. The overall relative error $\boldsymbol{E}$ is given parenthetically for the each result.*

5. Conclusion. We have presented an algorithm to implement series approximations that is adaptive in the ϵ. Using this algorithm, we are able to obtain accurate results at a reduced computational cost. By quantifying the way the coefficients decayed, we approximated the interval of convergence.

In our numerical results, we observed that if there is a smaller interval length, smaller N values are sufficient to have a more accurate approximation, which is consistent with other numerical methods. A more thorough investigation to quantify this relationship is underway. This would lead to an algorithm that is not only adaptive in the ε, but also in the number of terms that is needed.

In more detailed models, parameters are not constant. It remains open to quantify

how the system performs when parameters are variable including incorporating birth and death rates into the models as in [15].

6. Acknowledgements. We would like to acknowledge the funding support of this project by Monmouth University's School of Science as part of the annual Summer Research Program.

REFERENCES

[1] F. Brauer, C. Castillo-Chavez, and Z. Feng, *Mathematical models in epidemiology*, vol. 69 of Texts in Applied Mathematics, Springer, New York, 2019, https://doi.org/10.1007/978-1-4939-9828-9, https://doi.org/10.1007/978-1-4939-9828-9. With a foreword by Simon Levin.

[2] J. Ghosh, U. Ghosh, and S. Sarkar, *Qualitative analysis of both hyperbolic and non-hyperbolic equilibria of a sirs model with logistic growth rate of susceptibles and inhibitory effect in the infection*, Computational Methods in Science and Technology, 24 (2018), pp. 285–300, https://doi.org/10.12921/cmst.2018.0000029.

[3] A. Harir, S. Melliani, H. El Harfi, and L. S. Chadli, *Variational iteration method and differential transformation method for solving the SEIR epidemic model*, Int. J. Differ. Equ., (2020), pp. Art. ID 3521936, 7, https://doi.org/10.1155/2020/3521936, https://doi.org/10.1155/2020/3521936.

[4] T. Harko, F. S. N. Lobo, and M. K. Mak, *Exact analytical solutions of the susceptible-infected-recovered (SIR) epidemic model and of the SIR model with equal death and birth rates*, Appl. Math. Comput., 236 (2014), pp. 184–194, https://doi.org/10.1016/j.amc.2014.03.030, https://doi.org/10.1016/j.amc.2014.03.030.

[5] J.-H. He and X.-H. Wu, *Variational iteration method: new development and applications*, Comput. Math. Appl., 54 (2007), pp. 881–894, https://doi.org/10.1016/j.camwa.2006.12.083, https://doi.org/10.1016/j.camwa.2006.12.083.

[6] K. Heng and C. L. Althaus, *The approximately universal shapes of epidemic curves in the susceptible-exposed-infectious-recovered (seir) model*, Sci. Rep., 10 (2020), p. 19365.

[7] C. T. Kelley, *Numerical methods for nonlinear equations*, Acta Numer., 27 (2018), pp. 207–287, https://doi.org/10.1017/s0962492917000113, https://doi.org/10.1017/s0962492917000113.

[8] H. Ma, Q. Zhang, and X. Xu, *Positivity-preserving numerical method for a stochastic multi-group SIR epidemic model*, Comput. Methods Appl. Math., 23 (2023), pp. 671–694, https://doi.org/10.1515/cmam-2022-0143, https://doi.org/10.1515/cmam-2022-0143.

[9] M. R. Mohamed Elhia and E. Benlahmar, *Optimal controls of an sir model with delay in state and control variables*, Biomathematics, 17 (2013), pp. 1–7.

[10] M. K. Ottar N. Bjornstad, Katriona Shea and N. Altman, *The seirs model for infectious disease dynamics*, Nature Methods, 17 (2020), pp. 557–558.

[11] L. Perko, *Differential equations and dynamical systems*, vol. 7 of Texts in Applied Mathematics, Springer-Verlag, New York, third ed., 2001.

[12] M. Rafei, H. Daniali, and D. D. Ganji, *Variational interation method for solving the epidemic model and the prey and predator problem*, Appl. Math. Comput., 186 (2007), pp. 1701–1709, https://doi.org/10.1016/j.amc.2006.08.077, https://doi.org/10.1016/j.amc.2006.08.077.

[13] D. Smith and L. Moore, *The sir model for spread of disease - the differential equation model*, Infectious Disease Modelling, 79 (nd), pp. 1–4.

[14] H. Srivastava, I. Area, and J. Nieto, *Power-series solution of compartmental epidemiological models*, Mathematical Biosciences and Engineering, 18 (2021), pp. 3274–3290.

[15] P. van den Driessche, *Reproduction numbers of infectious disease models*, Infectious Disease Modelling, 79 (2017), pp. 288–303.